Low-cost nonlinear optics experiment for undergraduate instructional laboratory and lecture demonstration

Rozane de F. TurchielloLuiz A. A. Pereira and Sergio L. Gómez

Citation: American Journal of Physics **85**, 522 (2017); doi: 10.1119/1.4984808
View online: http://dx.doi.org/10.1119/1.4984808
View Table of Contents: http://aapt.scitation.org/toc/ajp/85/7
Published by the American Association of Physics Teachers

Low-cost nonlinear optics experiment for undergraduate instructional laboratory and lecture demonstration

Rozane de F. Turchiello
Department of Physics, Federal University of Technology of Paraná, Ponta Grossa 84016-210, Brazil

Luiz A. A. Pereira and Sergio L. Gómez[a)]
Department of Physics, Ponta Grossa State University, Ponta Grossa 84.030-900, Brazil

(Received 20 May 2016; accepted 18 May 2017)

This paper presents a simple and affordable experiment on the thermal lens effect, suitable for an undergraduate educational laboratory or as a tabletop demonstration in a lecture on nonlinear optics. Such an experiment exploits the formation of a lens in an absorbing medium illuminated by a laser beam with a Gaussian intensity profile. As an absorber, we use a commercial soy sauce, which exhibits a strong thermal lensing effect. Additionally, we show how to measure the radius of a Gaussian beam using the knife-edge method, and how to estimate the focal length of the induced thermal lens.
[http://dx.doi.org/10.1119/1.4984808]

I. INTRODUCTION

The teaching of optics at the undergraduate level usually focuses on the field of linear optics, in which it is assumed that light does not modify the optical properties of a medium. However, when the light field does modify the optical properties of the medium we say that a nonlinear optical effect occurs.[1] The field of nonlinear optics started shortly after the invention of the laser, and research in this field continues to evolve because of important developments from basic science and applied physics to technological applications. Nonlinear optical phenomena include harmonic generation, frequency mixing, and nonlinear optical absorption, among others.[2] An important set of nonlinear optical phenomena that originate from the dependence of the refractive index on the intensity of light includes the optical Kerr effect and the thermal lens effect.[3,4] The major drawbacks for introducing the subject of nonlinear optics into the undergraduate classroom are that it is a difficult topic and that the necessary apparatus for visualizing a nonlinear optical effect may not be affordable.

The emergence of a nonlinear optical effect depends on characteristics of the laser beam, such as intensity and pulse length, and on the physical properties of the medium, such as symmetry and optical absorption. Previous works have presented experiments for observing different nonlinear optical effects employing specific systems and experimental conditions that are not usually found in instructional laboratories.[5–8] The thermal lensing effect, as presented here, is an affordable apparatus and has a relatively simple theoretical background for undergraduate students. Such an effect is based on the formation of a refractive index gradient in an absorbing medium, which is caused by a induced thermal gradient that results when a Gaussian beam traverses the material. In this paper, we present a simple and inexpensive experimental setup for visualizing this nonlinear optical effect. The experiment uses commercial soy sauce, which is a highly absorbing medium, and can be easily found in supermarkets. We will first provide an introduction to the Gaussian beam and the thermal lens effect. Then, we provide a step-by-step procedure for observing the thermal lens effect, and list instructions on how to determine the focal length of this lens.

II. THEORETICAL BACKGROUND

A. Gaussian beam

Typically, commercial lasers have a beam with a spatial profile that corresponds to the Gaussian or TEM_{00} mode, the fundamental mode of an optical oscillator and the closest representation to the notion of a "ray" of light in geometrical optics.[9] The mathematical expression of the intensity of the Gaussian beam is given by

$$I(r) = I_0\, e^{-r^2/w^2}, \tag{1}$$

where r is the distance from the propagation axis, I_0 is the intensity on this axis (where $r=0$), and w is the radial distance at which the intensity has decreased to $1/e$ of its axial or peak value (the beam radius). For a focussed Gaussian beam propagating along the z-axis, the beam radius is given by

$$w(z)^2 = w_0^2\left[1+\left(\frac{\lambda z}{2\pi w_0^2}\right)^2\right],$$

where w_0 is the beam waist (the beam radius at the focus, $z=0$) and λ is the wavelength of the laser beam. Figure 1 shows the spatial distribution of a Gaussian beam; panel (a) shows a cross section of the beam and panel (b) shows a 3D intensity profile in arbitrary units.

B. Thin spherical lens

A lens is a refracting material that modifies the path of an incident wave by introducing a phase delay $\Delta\phi(x,y) = knl(x,y)$, where $k = 2\pi/\lambda$ is the wavenumber, n is the refractive index of the lens material, and $l(x, y)$ is the thickness of the medium at the point (x, y). The profile of the lens determines its focusing properties, and for a thin spherical lens of focal length f, the profile is given by $l(x,y) \propto -(x^2+y^2)/f$.[10] Thus, if a plane wave of unit amplitude $E_i = e^{i\phi}$ is normally incident on a thin spherical lens of focal length f, the optical field just behind the lens, E_f, neglecting the constant phase factor, will be

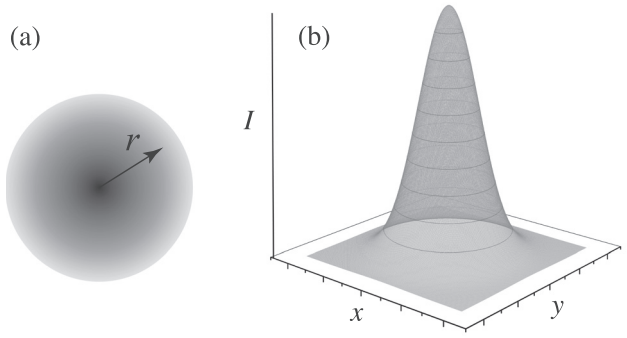

Fig. 1. (a) Sketch of the spot of a Gaussian beam on a screen; r is the radial distance from the center of the beam, which propagates along the z-axis. (b) A 3D plot of the intensity I of a Gaussian beam with a maximum at $x = y = 0$ ($r = 0$).

$$E_f = e^{-ik(x^2+y^2)/2f} = e^{-ikr^2/2f}. \tag{2}$$

We can interpret the exponent here as a paraxial spherical wave. Indeed, a spherical wave is given by $e^{\pm ikR}/R$, where R is the radius of curvature, and the sign corresponds to an outward (+) or inward (–) moving spherical wave.

By considering a spherical wave propagating along the z-axis, with the source or sink at $z = 0$, and for points on the wavefront close to the z-axis (the paraxial approximation), the distance R can be approximated as

$$\begin{aligned} R &= \sqrt{x^2+y^2+z^2} = z\sqrt{\frac{x^2+y^2}{z^2}+1} \\ &\approx z\left(1+\frac{r^2}{2z^2}\right) = z+\frac{r^2}{2z}. \end{aligned} \tag{3}$$

Thus, in the paraxial approximation with $z \approx R$, the expression for a spherical wave can be written as

$$\frac{e^{\pm ikR}}{R} \propto e^{\pm ikr^2/2R}. \tag{4}$$

Comparing Eq. (2) with Eq. (4), it is evident that, for a thin lens with $f > 0$, the (spherical) wave will converge to a point a distance f to the right of the lens and for $f < 0$, it will diverge from a point a distance f to the left of the lens. Figure 2 depicts the effect of a diverging lens on the wavefront of an incident plane wave.

C. Quadratic medium

The index of refraction of a medium is a dimensionless parameter that is inversely proportional to the speed of light in the medium, and generally depends on the frequency of the optical field (dispersion)[11] and can also depend on temperature.[12] We will now show that a material with uniform thickness b and nonuniform refractive index $n(x, y)$ can refract light in a manner similar to a lens. We assume a medium of uniform thickness l and refractive index given by $n(r) = n_0 + \delta r^2$ (a quadratic medium), where n_0 and δ are constants. Considering again a normally incident plane wave of unit amplitude $E_i = e^{i\phi}$ on the sample, the optical field behind the lens will be

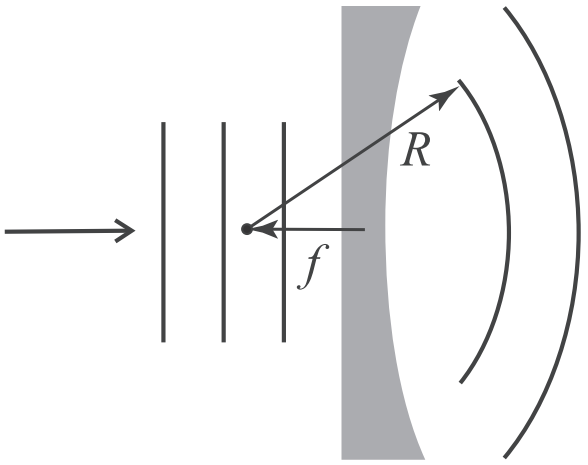

Fig. 2. The effect of a diverging lens of focal length f on an incident plane wave is to produce a spherical wave diverging from a point at a distance f to the left of the lens.

$$\begin{aligned} E_f &= E_i e^{i\Delta\phi} = e^{i(\phi+\Delta\phi)} \\ &= e^{-i\left[\phi+kb(n_0+\delta r^2)\right]} \\ &\propto e^{-ikb\delta r^2}. \end{aligned} \tag{5}$$

Comparing Eq. (5) with Eq. (2), we see that the wavefront of the wave just behind the quadratic medium is a paraxial spherical wave with a focal length $f \propto \delta^{-1}$. Thus, the sign of δ will determine whether the lens is converging or diverging.

D. Thermal lens

It is experimentally observed that a change in temperature leads to a change in the refractive index of a medium. If the refractive index of a medium at temperature T is $n_0(T)$, the value of the index of refraction at temperature $T + \Delta T$ can be written as[12,13]

$$n(T+\Delta T) = n_0(T) + \frac{dn}{dT}\Delta T, \tag{6}$$

where dn/dT is the thermo-optic coefficient. When light traverses an absorbing medium, the absorbed electromagnetic energy from the beam is partially converted into heat by a non-radiative relaxation process, which leads to heating of the medium. By supposing that the heat produced per unit length, $Q(r)$, is proportional to the intensity $I(r)$, and that the heat flux is radial only, it is possible to show[14] that ΔT depends on r^2. That is, a temperature gradient with radial symmetry is established in the medium and hence a gradient of refractive index with the same symmetry is established from Eq. (6). The net result is a thermal "lens" that transforms a plane wave as given in Eq. (2).

Typical values of the thermo-optic coefficients are on the order of $10^{-5}/^{\circ}$C. By assuming a paraxial propagation of the beam, it is admissible to approximate the Gaussian function in Eq. (1) by a Taylor series expansion around $r = 0$, which leads to a quadratic dependence on r. Thus, to lowest order, the refractive index and the optical path $\Gamma = bn(r)$ followed by a ray through the sample of uniform thickness b are both quadratic functions of r. In the paraxial approximation, the sample thus behaves like a spherical lens. Gordon *et al.*[14] showed that the focal length f_{th} of the induced thermal lens is

a function of time, and that after a transient period of several milliseconds for liquids, this focal length can be written

$$f_{\text{th}} \propto \frac{n_0 \kappa w^2}{P_0 b \alpha (dn/dT)}, \tag{7}$$

where P_0 is the power of the laser beam, κ is the thermal conductivity (in W/cm °C), α is the optical absorption coefficient (in cm^{-1}), and w is the radius of the Gaussian beam at the position of the sample.[14] The induced thermal lens will be converging ($f_{\text{th}} > 0$) when $dn/dT > 0$ and diverging ($f_{\text{th}} < 0$) when $dn/dT < 0$ (see Fig. 3). The stronger the lens the shorter the focal length.

III. EXPERIMENTAL DETAILS

A. Experimental setup

As a medium for observing the nonlinear optical phenomenon of thermal lensing, it is proposed to use commercial soy sauce, a fluid that has an intense optical absorption in the visible range of the electromagnetic spectrum. As a control medium, tap water can be used. The experimental setup includes a laser with a Gaussian intensity profile (a Gaussian beam), a converging lens, and a screen. Figure 4 shows a schematic of the experimental setup which can be placed on a table. The purpose of the converging lens is to increase the intensity of the beam, allowing for better visualization of the thermal lens effect. In our experimental setup, we used a He-Ne laser ($\lambda = 632.8$ nm) of about 15 mW and a converging lens of focal length $f = 8.9$ cm.

The soy sauce and the control medium can be encapsulated into submillimeter-thick glass cells made from microscope slides. To make a cell, begin by using a glass cutter to cut two equal pieces from the microscope slides, with sides lengths ∼2 cm. Next, cut a thin film (∼200-μm thick) of Teflon or plastic in the shape of a letter "U," which will act as a spacer for the slabs of glass. Finally, affix the spacer between the glass slabs using an epoxy resin (Fig. 5). Once dry, the cells are filled with the fluids using a Pasteur pipette.

The experimental procedure consists of exploring the optical response of the sample and the control medium at different positions near the focus of the lens by observing the laser spot on a screen positioned in the far-field region. At minimum, three different positions should include: (i) far from the focus of the lens, where the intensity of the laser is rather low (the waist of the Gaussian beam is large so the energy is spread out over a large area), as well as (ii) right before and (iii) right after the focus of the lens, where the intensity of the beam is rather high.

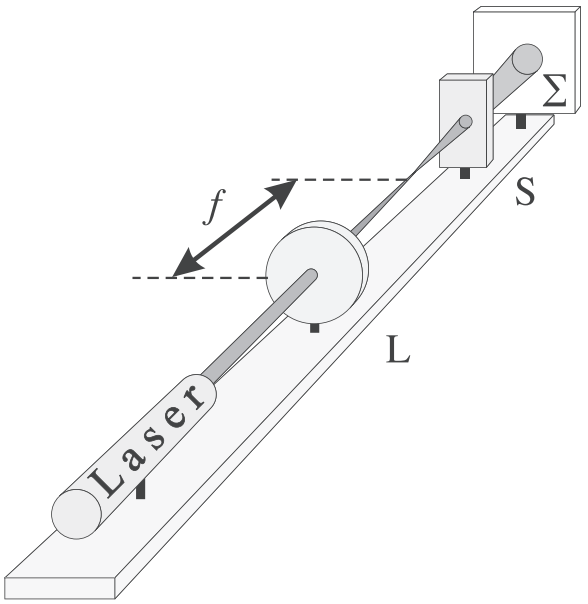

Fig. 4. Sketch of the experimental setup for observing thermal lensing: lens (L) with focal length f, sample (S), and screen (Σ).

B. Measurement of the beam radius by the knife-edge method

As a quantitative analysis of the thermal lens effect, it is proposed to measure the radius of the Gaussian beam at a position z along the propagating axis using the knife-edge method. The method consists of measuring the power of the beam while a sharp edge (such as a razor blade on a linear stage with a micrometer) is scanned along a direction perpendicular to the z-axis. The power of the unblocked portion of the beam is recorded as a function of the position of the blade, from which it is possible to reconstruct the spatial profile of the Gaussian beam at the position z. The general setup of this technique is shown in Fig. 6.

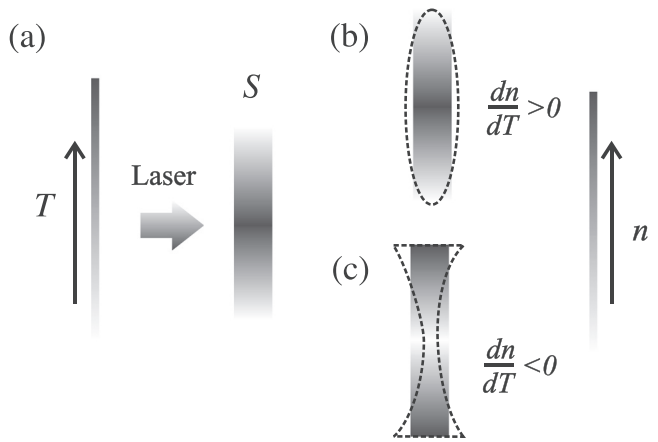

Fig. 3. (a) The spatial profile of the temperature in a sample S is shown in grayscale. The spatial profile of the refractive index is shown in grayscale for both positive (b) and negative (c) thermo-optic coefficients.

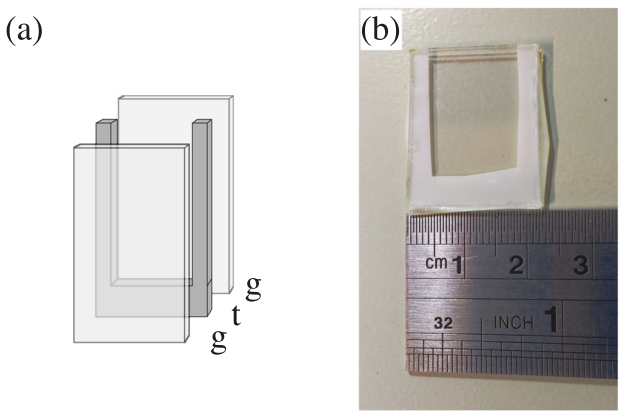

Fig. 5. (a) Sketch of a cell composed of two pieces of glass (g) from a microscope slide and spacer (t). (b) Photograph of the finished cell using Teflon film as a spacer.

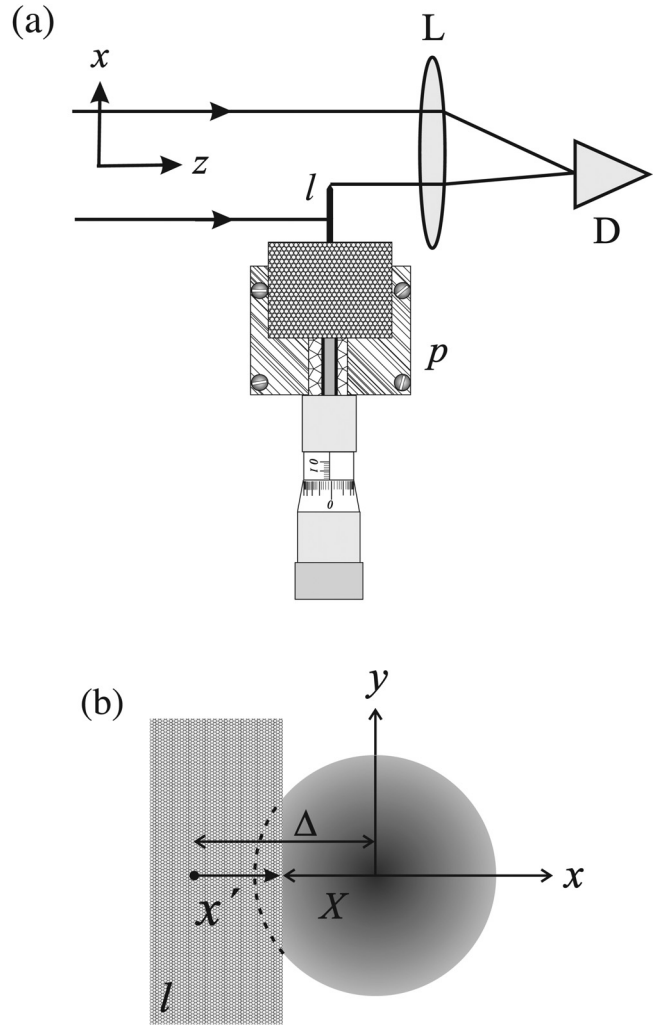

Fig. 6. (a) Experimental setup of the knife-edge technique: converging lens (L), razor blade (l), linear stage with micrometer screw (p), and photodetector (D). (b) An axial view of the knife edge and beam helps define the variables in Eq. (8).

For each position X of the blade, the power of the unblocked portion of the beam is given by

$$P(X,z) = \frac{P_0}{\pi w^2(z)} \int_X^{+\infty} e^{-x^2/w^2(z)} dx \int_{-\infty}^{+\infty} e^{-y^2/w^2(z)} dy = \frac{P_0}{\sqrt{\pi} w(z)} \int_X^{+\infty} e^{-x^2/w^2(z)} dx. \tag{8}$$

The last integral is related to the error function, giving the final result

$$P(X,z) = \frac{P_0}{2} \operatorname{erfc}\left(\frac{X}{w(z)}\right), \tag{9}$$

where the complementary error function defined as[15]

$$\operatorname{erfc}(x) \equiv 1 - \operatorname{erf}(z) = \frac{2}{\sqrt{\pi}} \int_x^{\infty} e^{-t^2} dt. \tag{10}$$

The function $\operatorname{erfc}(x)$ has a maximum value of 2 as $x \to -\infty$ and decreases monotonically with x, reaching its minimum value of 0 as $x \to \infty$. Some specific values of this function are: $\operatorname{erfc}(0) = 1$, $\operatorname{erfc}(1) = 0.1573\ldots$, and $\operatorname{erfc}(-1) = 1,8427\ldots$. Thus, the values of $\operatorname{erfc}(x)$ at $x = -1$ and $x = 1$ correspond to approximately 92% and 8% of its maximum, respectively. To work around knowledge of the value of X, we define a new variable by $x' = X + \Delta$, where Δ is chosen so that at $x' = 0$, the starting point of the scanning, the beam is completely unblocked. We can then write

$$P(x',z) = \frac{P_0}{2} \operatorname{erfc}\left(\frac{x' - \Delta}{w(z)}\right). \tag{11}$$

The signal given by the photodetector $V(x',z)$ when at position z with the blade at position x' will be proportional to $P(x',z)$. There are two ways to obtain $w(z)$ from $V(x',z)$. The first way is to determine the values of x' where the signal $V(x',z)$ is $\sim$8% and $\sim$92% of its maximum value, denoted as $x'(8\%)$ and $x'(92\%)$, respectively. From the properties of the $\operatorname{erfc}(x)$ function, it can then be determined that $2w = x'(8\%) - x'(92\%)$. The second way is based on the derivative of $P(x',z)$. By the fundamental theorem of calculus,[16] we have that

$$-\frac{dP}{dx'} \propto e^{-(x'-\Delta)^2/w^2(z)}, \tag{12}$$

showing that $-dP/dx'$ is proportional to a Gaussian function of the same width as the intensity I. The derivative of the data can be performed using an algorithm such as

$$\frac{dy}{dx} = \frac{1}{2}\left(\frac{y_{i+1} - y_i}{x_{i+1} - x_i} + \frac{y_i - y_{i-1}}{x_i - x_{i-1}}\right), \tag{13}$$

with any spreadsheet or by any available data analysis program. One can then estimate w by finding the x' values for which $-dP/dx'$ is about $1/e$ of the maximum. Another possibility would be to fit a Gaussian function to determine w.

C. Determining the focal length of the thermal lens

An appropriate parameter for describing a Gaussian beam is the complex curvature, or complex size parameter q, given by[9,17]

$$\frac{1}{q} = \frac{1}{R} - i\frac{\lambda}{\pi w_E^2}, \tag{14}$$

where R is the radius of curvature of the beam and w_E is radius of the Gaussian amplitude of the electric field.[18] When a beam propagates through an optical system composed of spaced lenses, the value of q at the entrance (q_1) and the exit (q_2) are related by

$$q_2 = \frac{Aq_1 + B}{Cq_1 + D}, \tag{15}$$

or

$$\frac{1}{q_2} = \frac{D/q_1 + C}{B/q_1 + A}, \tag{16}$$

where A, B, C, and D are the elements of the $ABCD$ matrix (or transfer matrix) that represents the optical system. For a propagation in air a distance d, the transfer matrix is

$$\mathbb{S} = \begin{bmatrix} 1 & d \\ 0 & 1 \end{bmatrix}, \tag{17}$$

and for a thin lens of focal distance f, the transfer matrix is

$$\mathbb{L} = \begin{bmatrix} 1 & 0 \\ -1/f & 1 \end{bmatrix}. \tag{18}$$

When a beam traverses an optical system formed by many spaced refractive devices, the representative matrix of the system is obtained by multiplying the matrix of each element, $\mathbb{S}$ or $\mathbb{L}$, in the sequence of the beam path. Therefore, the focal length of the induced lens in the sample at a determined position can be estimated by evaluating the imaginary part of the reciprocal of q_2, namely, $\mathrm{Im}(1/q_2) = -\lambda/\pi w_{E,2}^2$, by Eqs. (16) and (14).

IV. RESULTS AND DISCUSSION

Figure 7 shows pictures of the spot of the laser on a screen, positioned approximately one meter from the lens, when the laser beam traverses the sample of soy sauce (left column) and tap water (right column). The rows in Fig. 7 show laser spot images when the sample is positioned far (∼50 cm) from the focus (top), right after the focus (middle), and right before the focus (bottom). The optical absorption of water in the visible part of the electromagnetic spectrum is negligible, so the laser beam does not induce a thermal lens with water. Therefore, the size of the spot does not depend on the position of the control [Figs. 7(a), 7(c), and 7(e)].

Meanwhile, Fig. 7(b) shows the spot when the cell containing soy sauce is far from the focus. Besides some bright dots of a granular, rather chaotic and disordered interference pattern (speckle) from density inhomogeneity of the sample,[19] the circular central part of the spot has the same size as that observed with the control medium. Far from the focus, the low intensity of the laser induces an insignificant thermal gradient. Contrast this with Figs. 7(d) and 7(f), which show the laser spot when the sample is positioned right after and right before the focus, respectively. At these positions, the higher intensity can induce a thermal lens, modifying the profile of the beam. With the sample right after the focus, the spot size is larger than that obtained by placing the sample far from the focus. On the other hand, with the sample right before the focus, the spot size is smaller. These observations can be understood by supposing that the laser beam induces a negative or diverging thermal lens as illustrated in Fig. 8. A diverging lens placed before the focus of the converging lens will focus the beam at a further away, reducing the size of the spot on the screen. Conversely, placing the diverging lens after the focus will cause the beam to further diverge, increasing the spot size.

It is worth noting that the formation of a thermal lens in the soy sauce can be observed with the unaided eye with a laser of at least 8 mW. For lower power lasers, in order to visualize the effect with the unaided eye, one could use a converging lens with a tighter focal length or a thicker sample. The sensitivity of the eye is usually lower than that of the photodetector so it is possible to demonstrate the formation of the thermal lens through the procedure discussed in Secs. III B and III C.

As an example of this procedure, Fig. 9(a) shows experimental data of the photodetector signal (voltage, V) read with a multimeter, as a function of the knife edge position x', for the beam right after the window of the laser. Figure 9(b) shows the derivative of the photodetector signal, $-dV/dx'$,

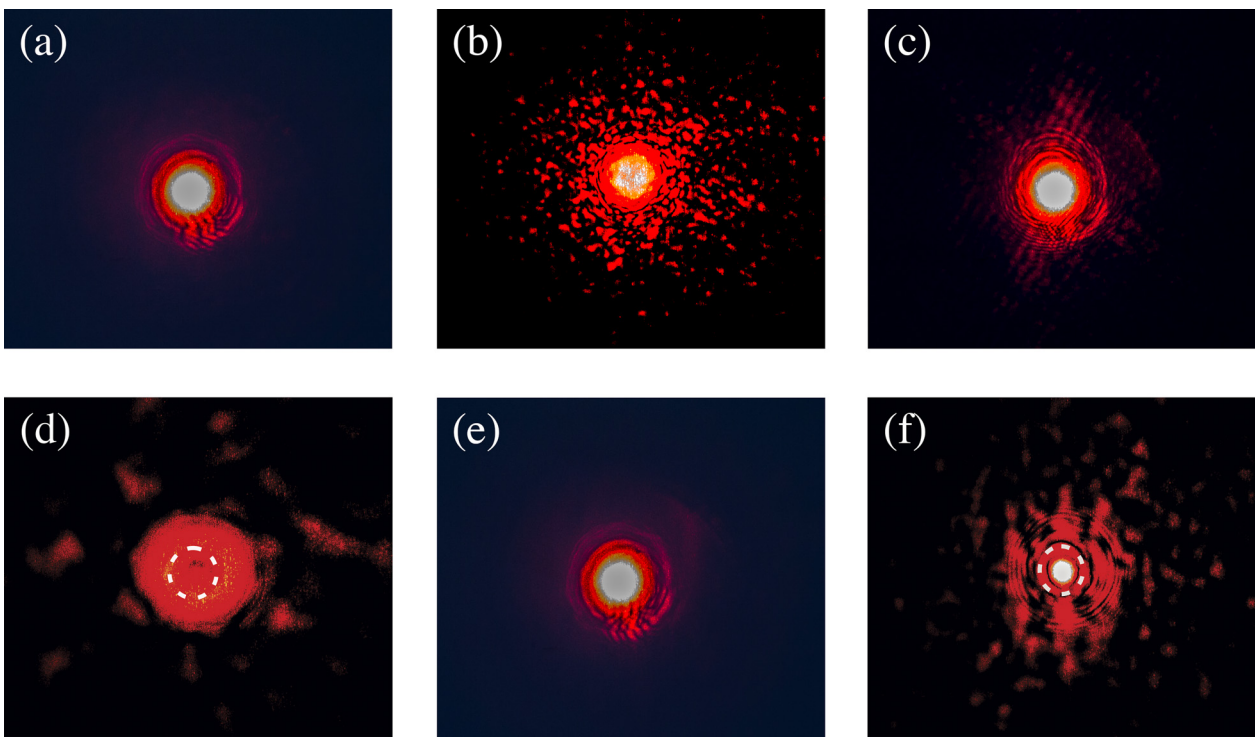

Fig. 7. Pictures of the laser spot on a screen. Panels (a), (c), and (e) show the laser spot when a cell containing pure water is placed far from the focus, right after the focus, and right before the focus, respectively. Panels (d)–(f) show the laser spot when a cell containing soy sauce is placed far from the focus, right after the focus, and right before the focus, respectively. For comparison, the dashed lines indicate the laser spot on the screen when the sample is positioned far from the focus, as determined by the eye's sensitivity.

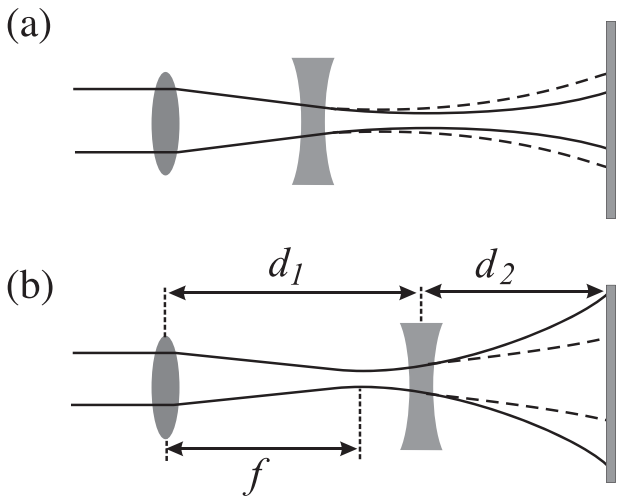

Fig. 8. Laser beam profile. The solid lines depict the actual profile of the beam when the sample, shown as a diverging lens, is placed (a) before and (b) after the focal point of the converging lens (focal length f). The dashed lines depict the profile the beam would have if the sample was absent (or far from focal point).

from the data shown in Fig. 9(a). Figure 9(b) also shows a Gaussian fit (solid curve) to the data. As can be seen, the Gaussian is shifted from $x' = 0$. From the fitting data, the width of the beam right after the window of the laser is about $w = 0.267 \pm 0.004$ mm.

Figure 10(a) shows the photodetector signal obtained by the knife-edge method at a distance $L = 36.8 \pm 0.2$ cm from the lens. The scanning was performed for two positions of the sample near the focus: when the sample was at a distance $d_{1,\mathrm{BF}} = 5.0 \pm 0.2$ cm after the lens (before the focus, BF), and when the sample was at a distance $d_{1,\mathrm{AF}} = 11.3 \pm 0.2$ cm after the lens (after the focus, AF). The scanning was also performed for the control medium (water, w). It is worth mentioning that for the control, the result of the scanning does not depend on its position near the focus. The uncertainty of the measurements is approximately the same size as the symbols. Figure 10(b) shows the derivatives of the curves displayed in Fig. 10(a). A fitting of the derivatives to a Gaussian function gave the following values for w: $w_{BF} = 0.46 \pm 0.02$ mm, $w_{AF} = 1.98 \pm 0.17$ mm, and $w_w = 0.90 \pm 0.03$ mm.

The *ABCD* (transfer) matrix that represents the optical system in our experimental setup can be obtained by the following product of matrices:

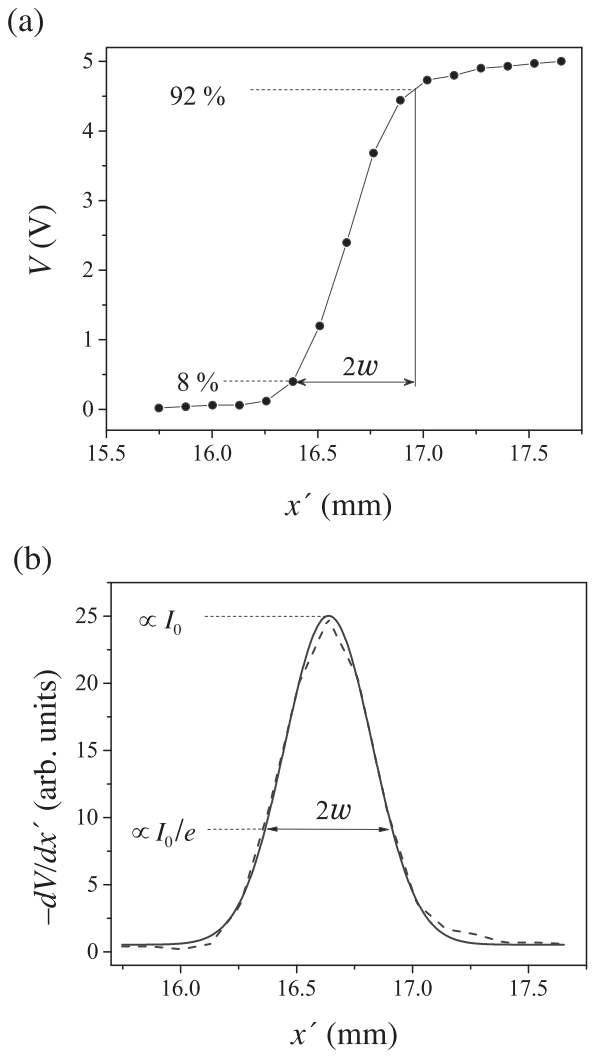

Fig. 9. (a) Plot of the photodetector signal $V(x', z)$, which is proportional to the power of the unblocked part of the beam, as a function of the blade's position. (b) Derivative of the data from panel (a) (dashed) and a Gaussian fit (solid).

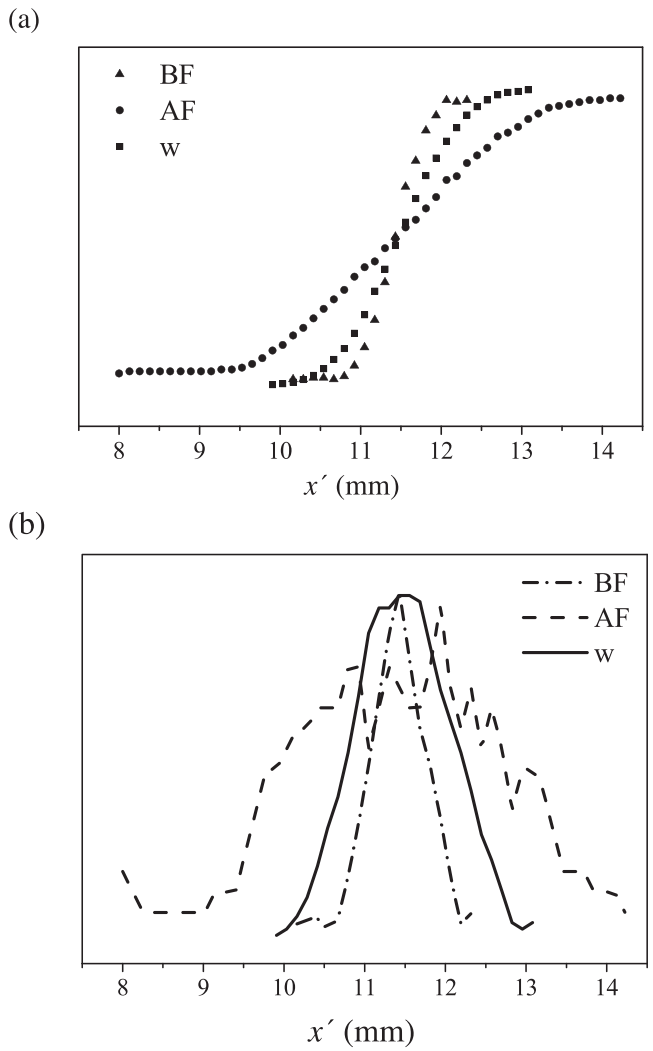

Fig. 10. (a) Normalized photodetector signal $V(x', z)$ for water (w) and for the sample when placed before the focus (BF) and after the focus (AF). (b) Normalized curves of the derivative of $V(x', z)$.

$$\begin{bmatrix} A & B \\ C & D \end{bmatrix} = \begin{bmatrix} 1 & d_2 \\ 0 & 1 \end{bmatrix} \begin{bmatrix} 1 & 0 \\ -1/f_{\text{th}} & 1 \end{bmatrix} \begin{bmatrix} 1 & d_1 \\ 0 & 1 \end{bmatrix} \begin{bmatrix} 1 & 0 \\ -1/f & 1 \end{bmatrix}. \tag{19}$$

From left to right, these matrices represent: propagation in air a distance d_2 from the sample to the plane that is located at the precision linear stage with the razor blade; a refraction at the sample that behaves as a (thin) lens of focal length f_{th}; a propagation in air a distance d_1 from the lens to the sample; and a refraction at the positive lens of focal length f (see Fig. 8). The Gaussian beam that emerges from the laser is diverging and its beam waist is located at the window of the laser, so for the Gaussian beam at the laser's window $R \to \infty$ and the complex curvature parameter is purely imaginary. Then, when the converging lens is positioned close to the laser's window, the parameter q for the beam at the left of the converging lens is approximately given by[18]

$$\frac{1}{q_1} = -i\frac{\lambda}{2\pi w_1^2}, \tag{20}$$

where w_1 is the waist of the beam at the left of the positive lens. In our experimental setup, $d_1 = 11.3 \pm 0.2$ cm, $d_2 = 25.5 \pm 0.2$ cm, and $f = 8.89$ cm. On the other hand, the waist of the beam emerging from the laser and at a distance d_2 from the sample as determined by the knife-edge method were $w_1 = 0.267 \pm 0.004$ mm and $w_2 = 1.9 \pm 0.2$ mm, respectively. The solution of Eq. (15), taking into account the matrix given in Eq. (19), leads to a quadratic equation, from which we select the negative root. In our case, the estimated focus of the induced lens at position d_1 is $f_{\text{th}} = -2.0 \pm 0.1$ cm.

In addition to soy sauce, other materials exhibit a strong negative induced thermal lens, such as ink, an aqueous solution of toner, and an aqueous solution of coffee. Materials that usually exhibit a large and positive value of the thermo-optic coefficient includes, for example, calamitic nematic liquid crystals with planar orientation when illuminated with light perpendicularly polarized to the alignment direction.[20]

V. CONCLUSIONS

In this paper, we showed that the thermal lens effect provides a fast, easy, and low-cost experiment for demonstrating the ability of light to self-modify its propagation through a medium. Such an experiment can be used in an undergraduate instructional laboratory as well as a tabletop demonstration to introduce the topic of nonlinear optics. In addition, such an experiment provides an opportunity for students to learn about a Gaussian beam, its properties, and its propagation through an optical system. Here, we proposed to use commercial soy sauce as an absorbing medium, which is safe and affordable, but it is also possible to employ other highly absorbing materials (e.g., ink, toner, etc.) for visualizing thermal lensing with the unaided eye.

ACKNOWLEDGMENTS

The authors acknowledge the National Institute of Science and Technology in Complex Fluids (INCT-FCx) and the Brazilian agencies CNPq, CAPES, and Fundação Araucária for financial support. The authors also thank Professor Gerson K. da Cruz and Professor Gelson B. de Souza for valuable assistance in preparing the figures.

[a]Electronic mail: sgomez@uepg.br

[1]Y. R. Shen, *Principles of Nonlinear Optics* (John Wiley & Sons, Hoboken, 2003).
[2]R. L. Sutherland, *Handbook of Nonlinear Optics*, 2nd ed. (Marcel Dekker, New York, 2003).
[3]R. W. Boyd, *Nonlinear Optics*, 3rd ed. (Academic Press, San Diego, 2008).
[4]R. D. Snook and R. D. Lowe, "Thermal lens spectrometry a review," Analyst **120**, 2051–2068 (1995).
[5]B. W. Payton and A. Sieradzan, "Two-quantum absorption: An undergraduate experiments in nonlinear optics," Am. J. Phys. **60**(11), 1033–1039 (1992).
[6]M. D. Matlin and D. J. McGee, "Photorefractive nonlinear optics in the undergraduate physics laboratory," Am. J. Phys. **65**(7), 622–634 (1997).
[7]S. McConville, D. Laurent, A. Guarino, and S. Residori, "Measurement of the giant nonlinear response of dye-doped liquid crystals," Am. J. Phys. **73**(5), 425–432 (2005).
[8]M. B. Kienlen, N. T. Holte, H. A. Dassonville, A. M. C. Dawes, K. D. Iversen, R. M. McLaughlin, and S. K. Mayer, "Collimated blue light generation in rubidium vapor," Am. J. Phys. **81**(6), 442–449 (2013).
[9]R. D. Guenther, *Modern Optics* (Wiley, New York, 1990).
[10]J. W. Goodman, *Introduction to Fourier Optics*, 2nd ed. (McGraw-Hill, New York, 1996).
[11]E. Hecht, *Optics*, 4th ed. (Addison Wesley, San Francisco, 2002).
[12]F. Simoni, *Nonlinear Optical Properties of Liquid Crystals and Polymer Dispersed Liquid Crystals*, Series on Liquid Crystals Vol. 2 (World Scientific, Singapore, 1997).
[13]S. E. Bialkowski, *Photothermal Spectroscopy Methods for Chemical Analysis*, Series of Monographs on Analytical Chemistry and its Applications Vol. 134 (John Wiley & Sons, New York, 1996).
[14]J. P. Gordon, R. C. C. Leite, R. S. Moore, S. P. S. Porto, and J. R. Whinnery, "Long transient effects in lasers with inserted liquid samples," J. Appl. Phys. **36**(1), 3–8 (1965).
[15]M. L. Boas, *Mathematical Methods in the Physical Sciences*, 2nd ed. (John Wiley & Sons, Hoboken, 1983).
[16]M. Spivak, *Calculus*, 3rd ed. (Publish or Perish, Houston, 1994).
[17]A. Gerrard and J. M. Burch, *Introduction to Matrix Methods in Optics* (Dover, New York, 1975).
[18]In textbooks on Gaussian optics, the spatial amplitude distribution of the electric field is given in terms of the Gaussian function e^{-r^2/w_E^2}, and the corresponding intensity is proportional to e^{-2r^2/w_E^2}. So the width of the Gaussian associated with the intensity as given in Eq. (1), w, and that of the electric field, w_E, are related by $w = w_E/\sqrt{2}$.
[19]J. W. Goodman, "Some fundamental properties of speckle," J. Opt. Soc. Am. **66**(11), 1145–1150 (1976).
[20]S. L. Gómez, V. M. Lenart, R. F. Turchiello, I. H. Bechtold, A. A. Vieira, and H. Gallardo, "Nonlinear optical properties of dye-doped E7 liquid crystals at the nematic-isotropic transition," Liq. Cryst. **43**(2), 268–275 (2016).